Dynamical and Energetic Properties of Hydrogen and Hydrogen-Tetrahydrofuran Clathrate Hydrates

Paul D. Gorman[1], Niall J. English[1,2,a)] and J.M.D. MacElroy[1]

[1]The SFI Strategic Research Cluster in Solar Energy Conversion, School of Chemical and Bioprocess Engineering and [2]Centre for Synthesis and Chemical Biology University College Dublin, Belfield, Dublin 4, Ireland.

Keywords: Molecular Dynamics, Dynamical Properties, Energetic Properties, Hydrogen Hydrate, THF Hydrate

Classical equilibrium molecular dynamics (MD) simulations have been performed to investigate the dynamical and energetic properties in hydrogen and mixed hydrogen-tetrahydrofuran sII hydrates at 30 and 200K and 0.05 kbar, and also at intermediate temperatures, using SPC/E and TIP4P-2005 water models. The potential model is found to have a large impact on overall density, with the TIP4P-2005 systems being on average 1 % more dense than their SPC/E counterparts, due to the greater guest-host interaction energy. For the lightly-filled mixed H_2-THF system, in which there is single H_2 occupation of the small cage (1s1l), we find that the largest contribution to the interaction energy of both types of guest is the van der Waals component with the surrounding water molecules in the constituent cavities. For the more densely-filled mixed H_2-THF system, in which there is double H_2 occupation in the small cage (2s1l), we find that there is no dominant component (*i.e.*, van der Waals or Coulombic) in the H_2 interaction energy with the rest of the system, but for the THF molecules, the dominant contribution is again the van der Waals interaction with the surrounding cage-water molecules; again, the Coulombic component increases in importance with increasing temperature. The lightly-filled pure H_2 hydrate (1s4l) system exhibits a similar pattern vis-à-vis the H_2 interaction energy as for the lightly-filled mixed H_2-THF system, and for the more densely-filled pure H_2 system (2s4l), there is no dominant component of interaction energy, due to the multiple occupancy of the cavities. By consideration of Kubic harmonics, there is some evidence of preferential alignment of the THF molecules, particularly at 200 K; this was found to arise at higher temperatures due to transient hydrogen bonding of the oxygen atom in THF molecules with the surrounding cage-water molecules.

[a)] Corresponding author. Tel: +35317161646. Email: niall.english@ucd.ie

INTRODUCTION

Gas hydrates are crystalline inclusion compounds with a H_2O lattice that forms a periodic array of cages with each cage large enough to contain a gas molecule[1,2]. There are three known hydrate structures: sI, sII and sH. Given our interest in hydrogen and tetrahydrofuran sII hydrates in this study, a unit cell in sII[3] hydrate consists of 136 water molecules forming six small cages and two large cages. The small cages are pentagonal dodecahedral (5^{12}) and the large cages are hexadecahedral ($5^{12}6^4$). Each 5^{12} cage may contain one, or possibly two, H_2 molecules, while each $5^{12}6^4$ cage may contain a single THF molecule or up to four H_2 molecules[4].

The possibility of using sII hydrates for hydrogen storage has been extensively studied[5-7]. The extreme pressure needed to form pure hydrogen hydrate has been a limiting factor and has led to the study of mixed stabiliser-H_2 hydrates[8,9,10], in the hope is that a stabilising compound will allow hydrate formation at lower pressures. Hydrates stabilised by THF have attracted interest in this respect as they have been reported to be stable at close to room temperature, and at much lower pressures than pure hydrogen-hydrate[4,5,8,11] Although the concept of large-scale seasonal storage is not new[12,13], the proposition of using mixed THF-H2 hydrate for such efforts[14] is attractive, as it is a completely reversible physical hydrogen storage material. However, the exact weight percentage of hydrogen in such a system is still disputed, with estimates ranging from 1-4 wt% H_2[8,14] greatly affecting its viability as a storage medium. It is understood that hydrate structures which enable multiple occupancy of hydrogen will likely be required for clathrate hydrates to be practical hydrogen storage medium. Ref. 15 presents part of a Tokyo-based feasibility study of on the large-scale *in situ* storage of hydrogen in the form of clathrate hydrates, in which it is concluded that a large portion of the energy that could be extracted from the hydrogen-hydrate would be needed to power the refrigeration required. However, their industrial design does not address the possibility of the geologic storage of hydrates where lower temperatures may be achieved at a lower energy cost.[15]

In the MD simulation of hydrates, there exists some uncertainty as to the exact effect of a fixed-

cage[5], in which the cage structure is immovable and the guest molecules are free, *versus* a flexible-cage[7], where the cage structure is free to distort. However, it is clear that there is a marked effect on energetic properties, for instance, from the differing guest-host interaction energies (-3.7 *versus* -2.2 kJ/mol for singly-occupied large cages) obtained in refs. 5 and 7. Despite this, the fixed-cage approach is increasingly used in simulations due to its relative simplicity[16-18].

In this study, we adopt an approach similar to that of ref. 7, *i.e.*, using rigid H_2O molecules, and allowing them to move freely, *i.e.*, no restrictions on cage motion. Given that the best available potential models for H_2 and mixed THF/H_2 hydrates are rigid-body, we use rigid-molecules for THF and H_2. The objective is to employ classical MD methods to scrutinise the guest translational and rotational dynamics and energetic interactions in pure hydrogen and mixed THF/H_2 hydrates with the water lattice, to determine the underlying factors governing their motion.

METHODOLOGY

A sII hydrate 1088-H_20 molecule supercell, consisting of 2x2x2 unit cells, with the fundamental unit cell length ~17Å[3] was constructed. The Bernal-Fowler rules[19] were used in selecting the initial orientation of the water molecules so that the total dipole moment would be vanishingly small, and the Rahman-Stillinger procedure was used to achieve a small total dipole moment[20]. Four systems were constructed, two of pure hydrogen hydrate (with quadruple occupation in the large cavities and single- and double-occupation in the small cages) and two of mixed THF/H_2 hydrate (again, with single- and double-occupation in the small cages by H_2). These systems are described further in Table I, along with the naming convention. The guests' initial positions in the system were generated by mass-centring, *i.e.*, by placing the THF centre-of-mass (COM) at the geometric cage centre, the THF molecules in the large cages, and mass-centring the singe H_2 molecules in the small cages (cf. Table I). For the cages containing multiple H_2 molecules, the molecules were arranged around the cage centre at an energetically reasonable distance from each other and the cage.

[insert Table I,II about here]

The water models used were SPC/E[21] and TIP4P-2005[22]. For THF and H_2, the Alavi *et al*. parameterisation[23] was used for the charges and Lennard-Jones (LJ) interactions, along with geometric combining rules $\varepsilon^0_{ij} = (\varepsilon^0_{ii}\varepsilon^{0j}_{j})^{½}$, $\sigma^0_{ij} = (\sigma^0_{ii}\sigma^0_{jj})^{½}$, for water-guest and guest-guest LJ interactions, for consistency with Alavi *et al*.

Equilibrium MD simulations were performed using DL-POLY 2. Long-range interactions were calculated via the Smoothed Particle Mesh Ewald method[24], and a van der Waals cutoff distance of 8 Å. Although this cutoff value is less than the standard 2.5σ value (which would be ~8.5Å in the 1s1l, 2s1l systems), this is not expected to qualitatively change the observed behaviour of the systems; although the densities may be affected slightly in quantitative terms, the trend of density variation with temperature would not be affected to any extent. Rigid constraints for the H_2O, THF and H_2 were employed which implement the NOSQUISH algorithm of Miller *et al*.[25], using velocity-Verlet[26] integration. 100 ps of Nosé-Hoover[27] NVT simulations were run at 30, 50, 100, 150, and 200K for each system with a 1 fs time-step, and a rather mild 0.5 ps thermostat relaxation time. These were followed by 100-400 ps NPT[28,29] runs at 0.05 kbar, with thermostat and barostat periods of 0.5 and 2 ps respectively, to allow each system volume to settle. NPT production runs, with the same thermostat and barostat, were performed on the relaxed 30 and 200K systems for a further 100 ps with a 2 fs time-step. These systems were then used to study guest and host translational dynamics, focusing on guest-host dynamical coupling, and also on guest-host interaction energies.

It should be pointed out that the use of classical MD to treat hydrogen molecules' motion, in particular, below around 150 K is approximate in nature, and the lack of provision of quantum effects like zero-point H_2 cage-rattling motions and quantisation of H_2 rotational motion, becomes less satisfactory at lower temperature. Bačić et al have studied these effects in much detail for

hydrogen-containing clathrates,[30-36] including explicit path-integral MD simulation;[36] based on these studies, it should be stressed that the classical MD results below 150 K reported in the present work needs to be interpreted with some caution due to the limitations of classical MD to describe accurately H_2 motion at low temperatures. Therefore, the present work seeks to describe only a classical approximation to hydrogen behaviour in clathrate systems, and seeks qualitative insights into dynamical and energetic properties; consequently, the results at 30, 50 and 100 K are necessarily somewhat tentative.

Normalised velocity auto-correlation functions (VACF's) measure the degree of significance of coupling of atomic motions with themselves. These were calculated for each atom type, *i*

$$Z(t) = \langle \mathbf{v}_i(0) \cdot \mathbf{v}_i(t) \rangle / \langle \mathbf{v}_i(0) \cdot \mathbf{v}_i(0) \rangle \quad (1)$$

The frequency modes of the VACFs contributing to motion are revealed via their power spectra (Fourier transforms).

Velocity cross-correlation functions (VCCFs) are defined as

$$J(t) = \langle \mathbf{v}_m(0) \cdot \mathbf{v}_n(t) \rangle \, / \, (\langle \mathbf{v}_m(0) \cdot \mathbf{v}_m(0) \rangle^{1/2} \langle \mathbf{v}_n(0) \cdot \mathbf{v}_n(0) \rangle^{1/2}) \quad (2)$$

where $m \neq n$. If the motions of guests are entirely localised and independent of lattice vibrations, the VCCF between guest and water will be damped rapidly and the Fourier transform (FT) of the VCCF will be featureless. On the other hand, if the motions of the water lattice and the guests are completely correlated, features in the FT of the VCCF will resemble the power spectrum of the individual components[37].

Electrostatic interaction energies of guests with the water lattice and the rest of the system were calculated using the Lekner method[38,39], and compared with the guests' van der Waals interaction energies, to ascertain if a dominant energy component exists, or if there is a subtle interplay between components. These were calculated separately for guest-water and guest-guest interactions, where the H_2 in the small and large cages are treated separately, and referred to as SH_2, and LH_2 respectively.

To study the possibility of preferred alignment of the guest molecules in the cages, the orientation

distribution function $f(\mathbf{r})$ is expanded in terms of the Kubic harmonics $K_n(r)$[40,41]

$$4\pi f(\mathbf{r}) = 1 + C_4K_4(\mathbf{r}) + C_6K_6(\mathbf{r}) + \ldots \quad (3)$$

where $\mathbf{r} = (x,y,z)$ is a unit vector specifying a direction of interest. In the case of THF, we have used the dipole moment vector, and in the case of H_2 we use the vector connecting the two hydrogen atoms. In eqn. 3, K_4 and K_6 refer to

$$K_4(\mathbf{r}) = (21/16)^{1/2}(5Q\text{-}3) \quad (4)$$

$$K_6(\mathbf{r}) = (13/128)^{1/2}(462R + 21Q\text{ -}17) \quad (5)$$

with $Q = x^4+y^4+z^4$ and $R = x^2y^2z^2$, $C_4 = \langle K_4 \rangle$ and $C_6 = \langle K_6 \rangle$. We calculate both $\langle K_4 \rangle$ and $\langle K_6 \rangle$ in the large and small cages[40]. A preferential alignment (*w.r.t.* the [100] cube axis) is given by non-zero $\langle K_4 \rangle$.

RESULTS AND DISCUSSION

The densities of the systems at 30, 50, 100, 150 and 200 K, with both potentials are shown in Fig. 1. The densities have a range of 841-1,108 kg/m^3, with about 1% greater density for TIP4P-2005 systems vis-à-vis the respective SPC/E cases. This is due to the higher electrostatic interaction energy in the TIP4P-2005 potential. We contrast the density of the 200 K SPC/E 1s1l system, 900 kg/m^3, with that of ref. 7, which measures the volumes of unit cells with fully-loaded large cages but empty small cages, using an SPC/E potential, giving a density of 971 kg/m^3. This suggests that even single-occupancy H_2 exerts an outward pressure on the cavity, increasing unit cell volumes and decreasing density.

[insert Figure 1 about here]

Selected host- and guest- power spectra (from VACFs) are shown in Figs. 2 and 3 for the SPC/E and TIP4P models for the mixed 1s1l system. For the host translational density of states (DOS), *i.e.*, the OW spectrum, it is thought[40,42-44] that the peak at about 60 to 100 cm^{-1} corresponds to

transverse acoustic phonons propagating along directions of high symmetry at the boundary of the Brillouin zone, while the higher frequency secondary peak at 300-400 cm^{-1} is thought to be attributable to longitudinal and transverse optical modes. The power spectra of the hydrogens in the water molecules of the host lattice, *i.e.*, the librational DOS, are depicted in the insets of Figs. 2 and 3 at 30 and 200 K; the librational density of states span the frequency range of 400 to 1250 cm^{-1}, and are separated from the translational DOS by a well-defined frequency gap. The temperature dependence of the spectra exhibits a circa 50 cm^{-1} shift between 30 and 200 K. The SPC/E potential model results are qualitatively similar to TIP4P-2005 potential, with the frequencies of the TIP4P-2005 potential shifted to higher frequencies by ~20 cm^{-1}; this may be attributable to slightly stronger hydrogen bonding within the host lattice for the TIP4P-2005 potential. For both the SPC/E and TIP4P-2005 potentials for the 1s1l system at 30 K, we see vibrational modes at 75 and 100 cm^{-1}, respectively, in the power spectra for the THF COM and OW (the water oxygen atom). At 200 K, we see the OW spectrum shift to 75cm^{-1} coinciding with that of THF. This is due to the larger extent of coupling to the cage of the THF's motion at 200 K (cf. Figs. 2 & 3) – this was verified directly by calculation of the THF-OW VCCF and their corresponding power spectra to identify strong similarity with the respective frequency modes in the THF and OW VACF power spectra, especially at 200 K (data not shown). This close coupling arises from the intimate steric contact of the THF with the surrounding large-cage water molecules, as will be discussed further below when considering THF-water energetic and hydrogen bonding interactions. The H_2 spectra (again, on a COM basis) depict certain overlap between both the host's lattice transverse acoustic and optical modes, but, at 200 K, move closer towards greater overlap with the lattice transverse acoustic mode, owing to greater collisions at higher temperature with the neighbouring cage-water molecules; this was confirmed by a greater overlap in the H_2-OW VCCF spectrum at 200 K. However, reductions in density at 200 K (cf. Fig. 1) do result in larger cage radii, and hence higher-temperature H_2-water coupling via greater thermal motion is moderated to some extent by larger radii.

[insert Figures 2 & 3 about here]

In the mixed 2s1l system, similar effects are observed for THF and the host librational DOS (not shown, for clarity). However, the double occupation of the small cage by H_2 leads to more collisions with the cavity, which is demonstrated via the higher correlation between the H_2 and the OW motion (cf. Fig. 4) in their VACF spectra at 30 and 200 K, especially with the host's longitudinal and transverse optical modes.

[insert Figure 4 here]

In Fig. 5, for the 1s4l pure-hydrogen system at 30 K with SPC/E (and TIP4P-2005, not shown), both the SH_2 and LH_2 (that is, the single H_2 in the small cavity and quadruple H_2 in the large cage) possess vibrational modes at about 230 cm^{-1}. At 200 K, the SH_2 vibrational modes shift downwards to about 150 cm^{-1}, closer to the lattice transverse acoustic mode (as for single-occupation of the small cage with THF at 200 K, cf. Fig. 3b) while the quadruple-occupation LH_2 modes remain at 230 cm^{-1}, in partial overlap between both lattice acoustic and optical modes. Again, greater higher-temperature H_2-water coupling is moderated by smaller system densities.

[insert Figure 5 here]

In Fig. 6, for the pure-hydrogen 2s4l system, a high degree of coupling is evident at 30K between double-occupation SH_2 and quadruple-occupation LH_2 with the lattice longitudinal and transverse optical modes at about 300 cm^{-1}. The tendency for H_2 vibrational coupling with lattice optical modes appears to be a signature of multiple H_2 occupation, for both large and small cages.

[insert Fig. 6 about here]

It is helpful to discuss briefly the variation in host phonon spectra in Figs. 2 to 6. In all cases, for the translational DOS, the transverse acoustic mode becomes more important at 200 K due to greater lower-frequency translational motion of the water oxygen atoms at higher temperature, which overlap to a greater extent with the guests' motion. The frequencies of the transverse acoustic and optical modes decrease by approximately 10 % at 200 K relative to 30 K. For pure hydrogen hydrate, the singly-occupied small cage system (1s4l) has a larger separation in frequency between the transverse acoustic and optical modes (~100 versus 350 cm^{-1}, cf. Fig. 5a) than the doubly-occupied small cavity (2s4l, ~120 versus 300 cm^{-1}, cf. Fig. 6a); this may be attributed to the greater interactions of the two H_2 molecules with the lattice leading to closer lattice translational modes. For mixed hydrates, a similar trend is seen in going from single- to double-occupation of the small cavity (1s1l having ~70 versus 300 cm^{-1} and 2s1l having ~80 versus 250 cm^{-1}, cf. Fig.s 2 b and 4b, respectively). At higher temperature, the librational DOS also shifts downward by circa 10 % in frequency, although the translational and librational DOS remain well separated. There is less dependence of the host librational spectra upon the nature and number of guests, due to distrinct separation between host-lattice translational and librational modes.

For the mixed 1s1l system, the most significant energy contribution originates from the guest-water van der Waals interactions in the surrounding cage, as shown in Fig. 7 for the SPC/E and TIP4P-2005 potentials. In contrast to this, we see a substantially wider distribution in the electrostatic interaction between the THF and water in the mixed double-H_2 occupation (2s1l) system, where it occurs at 30 and 200 K for SPC/E and 200K for TIP4P-2005 (Fig 8), suggesting that THF molecules may be adopting certain higher-energy positions transiently during rotation within their larger-radii cages. There is some evidence for this in Fig 9 where the THF has a $\langle K_4 \rangle$ value of -0.15 at 200 K suggesting preferential alignment in the cage, however there is no evidence for preferential alignment at 30 K, in contrast with H_2 which shows a high degree of preferential alignment at both temperatures.

[insert Figures 7-9 about here]

To investigate this behaviour of THF motion further, particularly at higher temperatures, hydrogen bonding between the oxygen atoms in THF molecules and the surrounding cage waters was studied, using similar methods to those reported previously for guest-host hydrogen bonding in H2S hydrates.[41] It was found that transient, sub-picosecond hydrogen bonding occurs for both potential models at 200 K, in agreement with the study of Alavi et al,[45] with persistence/existence lifetimes of circa 0.65 and 0.5 ps, taking place around 18 and 14 % of the time for TIP4P-2005 and SPC/E models, respectively. The greater extent of cage vibrations at 200 K allows for a greater overlap of host-oxygen and THF COM rattling modes vis-à-vis lower temperatures (cf. Fig. 2b versus Fig. 2a and also Fig. 3b versus Fig. 3a), and this allows for transient existence of hydrogen bonded states which break and reform repeatedly over sub-picosecond timescales, which favours the existence of preferred orientations at 200 K (cf. Fig. 9). The THF-host hydrogen bonded states lead to distinct electrostatic interaction energies as distinct to non-hydrogen bonded configurations, which helps to explain wider distributions of Coulombic interaction energies at 200 K (cf. Fig. 8a).

For the pure-hydrogen system 1s4l, the van der Waals contribution is large only for SH_2-water in all systems owing to a small cage, where it resembles the small cage from the single-occupation mixed hydrate (1s1l). This suggests that the guest molecule in the large cage has little direct impact on the small cage guest.

From the Kubic harmonics, there is some evidence for preferential alignment for the THF in the 1s1l system at both 30 and 200 K. $\langle K_4 \rangle$ increases in magnitude from approximately -0.05 at 30 K to -0.15 at 200 K for the SPC/E model, while the H_2 shows almost no preferential alignment at 30 K in the SPC/E and TIP4P model. However, they have a $\langle K_4 \rangle$ of ~0.08 and ~0.04 respectively at 200 K, suggesting that the effects of the water model are more pronounced at lower temperatures, and that the H_2 alignment may be highly influenced by the higher electrostatic interaction with the

water molecules for the TIP4P potential.

CONCLUSIONS

In this study, equilibrium MD simulations were carried out to investigate the classical energetic and dynamical properties in pure-hydrogen and mixed hydrates at 30 and 200K and 0.05 kbar, and also at intermediate temperatures, using SPC/E and TIP4P-2005 water models. The SPC/E and TIP4P-2005 potentials have a slight effect on densities, with the TIP4P-2005 systems being ~1% more dense than their SPC/E counterparts. The velocity correlation functions and spectra were also in semi-quantitative agreement with the SPC/E and TIP4P-2005 models.

The rattling motion of the guests in the large and small cages for the mixed 1s1l- and 2s1l-hydrates were around 75 cm^{-1} for THF and 200-300 cm^{-1} for H_2 at 30 K, with the singly-occupied small-cage H_2 rattling shifting downwards to around 150-225 cm^{-1} at 200 K, closer to the lattice acoustic modes. A signature of double-occupation of the small cage by H_2 is of strong coupling with the lattice optic modes, regardless of temperature. The rattling motion of THF in the large cage is overlapped markedly with the lattice acoustic modes, due to closer contact, as evidenced by prominent van der Waals interaction energy terms and string similarities of THF-OW VCCF spectra with their respective VACF spectra. This is particularly evident at higher temperatures, *e.g.*, 200 K, due to transient THF-water hydrogen bonding leading to strong coupling of modes.

Unsurprisingly, the major contributor of interaction energy for the mixed 1s1l-, 2s1l-hydrate systems is that with water molecules. On occasion, the electrostatic interaction between THF and water makes a significant contribution at higher temperatures, although the relatively widely distributed nature of this energy distribution (e.g., Fig. 8a) suggests that these energy states may be transient; the finding of transient THF-water hydrogen bonds at higher temperatures confirms this view. There is some evidence from the $\langle K_4 \rangle$ results of a certain degree of preferential alignment of the THF and, to a lesser extent, H_2, with THF values of -0.05 and -0.13 for 30 and 200 K, respectively, with the SPC/E model, and +0.04 and -0.17 for the TIP4P-2005 potential; this was

found to arise as a consequence of transient THF-water hydrogen bonding, which becomes more significant at higher temperatures.

The present findings, particularly those of THF-water hydrogen bonding which serve to confirm the earlier results of Alavi et al,[45] have characterised the energetic and dynamical properties of pure- and mixed-hydrogen hydrates and of how THF-water hydrogen bonding underlines these properties at higher temperatures. Given the importance of these systems as media for hydrogen storage, especially on a long-term or geologic-scale basis at amenable temperatures and pressures, this study has shown that MD methods are highly useful in assessing, even on a qualitative basis, their viability: in particular, the temperature-dependence of densities, and their values, is important for designing hydrogen storage systems' volumetric capacity, and the analysis of guest-host interaction energies as a function of composition will be of further use in determining the energetic viability of formation of these media. It is hoped that MD simulation, and the applicability of more accurate potential models, will evolve in sophistication to serve as a quantitatively accurate predictive, *in silico* design tool for assessing hydrogen storage in hydrates, particularly in mixed hydrogen hydrates using other guests, *e.g.*, THF, for lower-pressure stabilisation. Although quantum[30-35] and path-integral MD[36] techniques for greater low-temperature quantitative accuracy are certainly to be advocated, in addition to state-of-the-art polarisable potential models, as important directions in realistic, accurate MD simulation of hydrogen hydrates' energetic and dynamical properties, the present study serves to report novel analyses for these properties and enhance our understanding thereof, despite the drawbacks of a classical treatment, particularly below about 150 K.

ACKNOWLEDGEMENTS

We acknowledge useful discussions with J.C. Baratault, Ritwik Kavathekar, Ilian Todorov, Mike Ashworth and the MD-GRAPE team. We thank Science Foundation Ireland (Grant 07/SRC/B1160), the Irish Centre for High End Computing and the Complex Adaptive Systems Laboratory (UCD) for the provision of high performance computing facilities.

REFERENCES

[1] Y.F. Makogon, *Hydrates of Hydrocarbons,* PennWell Books, Tulsa, Oklahoma, 1997.

[2] E.D. Sloan and C.A. Koh, *Clathrate Hydrates of Natural Gases*, 3rd rev. ed., CRC Press, Taylor & Francis USA, 2007.

[3] G.A. Jeffrey and R.K. McMullan, *Prog. Inorg. Chem.*, 1967, **8**, 43–108.

[4] W.L. Mao, H. Mao, A.F. Goncharov, V.V. Struzhkin, Q. Guo, J. Hu, J. Shu, R.J. Hemley, M. Somayazulu and Y. Zhao, *Science*, 2002, **297**, 2247-2249.

[5] S. Patchkovskii and J.S. Tse, *PNAS*, 2003, **100**, 14645-14650.

[6] M.H.F Sluiter, H. Adachi, R.V. Belosludov, V.R. Belosludov and Y. Kawazoe, *Mater. Trans.*, 2004, **45**, 1452-1454, .

[7] S. Alavi, J.A. Ripmeester and D.D. Klug, *J. Chem. Phys*, 2005, **123**, 024507.

[8] H. Lee, J. Lee, D.Y. Kim, J. Park, Y.T. Seo, H. Zeg, I.L. Moudrakovski, C.I. Ratcliffe and J.A. Ripmeester, *Nature*, 2005**, 434**, 743-746, .

[9] T.M. Inerbaev, V.R. Belosludov, R.V. Belosludov, M. Sluiter, Y. Kawazoe, J. Kudoh, *J. Incl. Phenom. Macrocycl. Chem.*, 2004**, 48**, 55-60.

[10] H. Erfan-Niya, H. Modarress and E. Zaminpayma, *J. Incl. Phenom. Macrocycl. Chem.*, 2011**, 70**, 1-2, 227-239.

[11] L.J. Florusse, C.J. Peters and J. Schoonman, et al., *Science*, 2004, **306**, 469-471.

[12] E. Newson, TH. Haueter, P. Hottinger, F. Von Roth, G.W.H. Schere and TH.H.Schucan. *Inter. J. Hydrogen Energy 23*, 1998, **10**, 905-909.

[13] N.F. Grünenfelder, T.H. Schunan, *Inter. J. Hydrogen Energy 14*, 1989, **8**, 579-586.

[14] L.J. Rovetto, T.A. Strobel, K.C. Hester, S.F. Dec, C.A. Koh, K.T. Miller and E.D. Sloan, *FY Annual Progress Report*, 2006.

[15] T. Nakayama, S. Tomura, M. Ozaki, R. Ohmura and Y.H. Mori, *Energy Fuels*, 2010, 24, 2576–2588.

[16] M.Z. Xu, F. Sebastianelli and Z. Bacic, *J. Chem. Phys.*, 2008, **128**, 13-14.

[17] T.J. Frankcombe and G.J. Kroes, *J.Phys.Chem. C*, 2007, **111**, 13044-13052.

[18] S. Alavi and J.A. Ripmeester, *Angew. Chem., Int. Ed.*, 2007, **46**, 6102-6105.

[19] J.D. Bernal and R.H. Fowler, *J. Chem. Phys.*, 1933, **1**, 515.

[20] A. Rahman and F.H. Stillinger, *J. Chem. Phys.*, 1972, **57**, 4009-4017.

[21] H. J. C. Berendsen, J. R. Grigera, and T. P. Straatsma, *J. Phys. Chem.*, 1987, **91,** 6269 - 6271.

[22] J. L. F. Abascal, and C. Vega, *J. Chem. Phys.*, 2005, 123, 234505.

[23] S. Alavi, J.A. Ripmeester and D.D. Klug, *J. Chem. Phys.*, 2006, **124**, 014704.

[24] U. Essmann, L. Perera, M.L. Berkowitz, T. Darden, H. Lee and L.G. Pedersen, *J. Chem. Phys.*, 1995, **103**, 8577-8595.

[25] T. F. Miller, M. Eleftheriou, P. Pattnaik, A. Ndirango, D. Newns, and G. J. Martyna, *J. Chem. Phys.*, 2002, **116**, 8649-8659.

[26] M.P. Allen and D.J. Tildesley, *Computer Simulation of Liquids,* Oxford, 1987.

[27] W.G. Hoover, *Phys. Rev. A*, 1985, **31**, 1695-1697.

[28] H.C. Andersen, *J. Chem. Phys.*, 1980, **71**, 2384-2393.

[29] W.G. Hoover, *Phys. Rev. A*, 1986, **34**, 2499-2500.

[30] M. Xu, Y.S. Elmatad, F. Sebastianelli, J.W. Moskowitz and Z. Bačić, *J. Phys. Chem. B*, 2006, **110**, 24806.

[31] F. Sebastianelli, M. Xu, Y.S. Elmatad, J.W. Moskowitz and Z. Bačić, *J. Phys. Chem. C*, 2007, **111**, 2497.

[32] F. Sebastianelli, M. Xu, D.K. Kanan and Z. Bačić, *J. Phys. Chem. A*, 2007, **111**, 6115.

[33] M. Xu, F. Sebastianelli and Z. Bačić, *J. Phys. Chem. A*, 2007, **111**, 12763.

[34] M. Xu, F. Sebastianelli and Z. Bačić, *J. Chem. Phys.*, 2008, **128**, 244715.

[35] M. Xu, F. Sebastianelli and Z. Bačić, *J. Chem. Phys.*, 2008, **129**, 244706.

[36] A. Witt, F. Sebastianelli, M.E. Tuckerman and Z. Bačić, *J. Phys. Chem. C*, 2010, **114**, 20775.

[37] J.S. Tse and M.A. White, *J. Phys. Chem.*, 1988, **92**, 5006-5011.

[38] J. Lekner, *Physica A*, 1989, **157(2)**, 826-838.

[39] J. Lekner, *Physica A*, 1991, **176(3)**, 485-498.

[40] J.S. Tse, M.L. Klein and I.R. McDonald, *J. Chem. Phys.*, 1984, **81**, 6146-6153.

[41] N.J. English and J.S. Tse, *J. Phys. Chem. A*, 2011, **115**, 6266-6232.

[42] J.S. Tse, C.I. Ratcliffe, B.M. Powell, V.F. Sears and Y.P. Handa, *J. Phys. Chem. A*, 1997, **101**, 4491-4495.

[43] J.S. Tse, V.P. Shpakov, V.P. Murashov, V.R. Belosludov, *J. Chem. Phys.*, 1997, **107**, 9271-9275.

[44] J.S. Tse, M.L. Klein, I.R. McDonald, *J. Phys. Chem.*, 1983, **87**, 4198-4203.

[45] S. Alavi, R. Susilo and J.A. Ripmeester, *J. Chem. Phys.*, 2009, **130**, 174501.

1s1l • 128 H_2 in 128 small cages • 64 THF in 64 large cages	2s1l • 256 H_2 in 128 small cages, 2 in each • 64 THF in 64 large cages
1s4l • 128 H_2 in 128 small cages • 256 H_2 in 64 large cages, 4 in each	2s4l • 256 H_2 in 128 small cages, 2 in each • 256 H_2 in 64 large cages, 4 in each

Table I. The four systems used: 1s1l – singly occupied small and large cages; 2s1l – doubly occupied small cage and singly occupied large cage; 1s4l – singly occupied small cage and quadruple occupation in the large cage; 2s4l – doubly occupied small cage, quadruple occupation in the large cage.

	SPC/E	**TIP4P-2005**
$\mathbf{q_O/q_D}$	-0.8476 *e*	-1.1128 *e*
ε	0.155402 kcal/mol	0.18519 kcal/mol
σ	3.1660 Å	3.1589 Å
$\mathbf{r_{OH}}$	1.0 Å	0.9572 Å
<HOH	109.47°	104.5°

Table II. A comparison of the two water models, where q_O/q_D refers to the charge on the oxygen and the dummy site respectively, while r_{OH} refers to the oxygen-hydrogen bond length.

FIGURE CAPTIONS

Figure 1. A comparison of system densities and temperatures. T denotes TIP4P-2005, and S denotes SPC/E. 1s1l is the H_2-THF system with singly occupied small cages, and all large cages occupied by THF. 2s1l is the H2-THF system with doubly occupied small cages. 1s4l is the pure H_2 system with singly occupied small cages and quadruple occupation of the large cages. 2s4l is the pure H_2 system with doubly occupied small cages and quadruple occupation of the large cages.

Figure 2. Power spectra for the 1s1l system with the SPC/E potential at (a) 30, (b) 200 K. The guest spectra are on a COM-basis.

Figure 3. Power spectra for the 1s1l system with the TIP4P-2005 potential at (a) 30, (b) 200 K. The guest spectra are on a COM-basis.

Figure 4. Power spectra for oxygen and H_2 for the 2s1l system with the SPC/E model at (a) 30, (b) 200K. The H_2 spectra are on a COM-basis.

Figure 5. Power spectra for the 1s1l system with the SPC/E model at (a) 30, (b) 200 K. The guest spectra are on a COM-basis.

Figure 6. Power spectra for oxygen, SH_2 and LH_2 for the 2s4l system with the SPC/E model at (a) 30, (b) 200 K (water protons omitted). The H_2 spectra are on a COM-basis.

Figure 7. Normalised probability distributions for interaction energies in the 1s1l system at 30 K with the SPC/E potential for H_2 with other H_2, with THF, and with water, for the (a) electrostatic component, and (b) van der Waals term.

Figure 8. Normalised probability distributions for interaction energies in the 2s1l system at 200 K with the TIP4P-2005 potential for H_2 with other H_2, with THF, and with water, for the (a) electrostatic component, and (b) van der Waals term.

Figure 9. Kubic harmonics in the 2s1l system with the TIP4P-2005 model at 200 K.

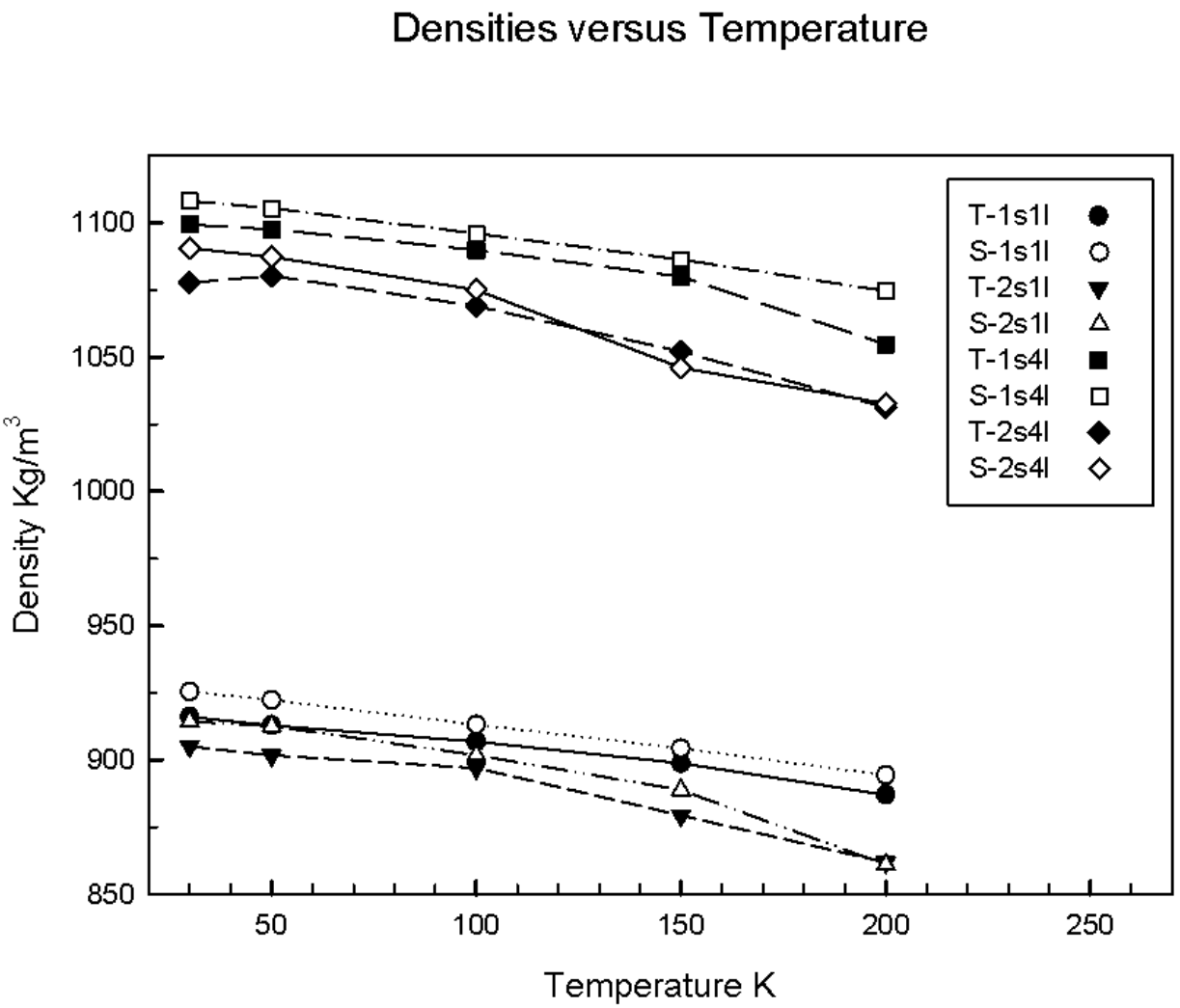

Fig. 1 System Density Comparison.

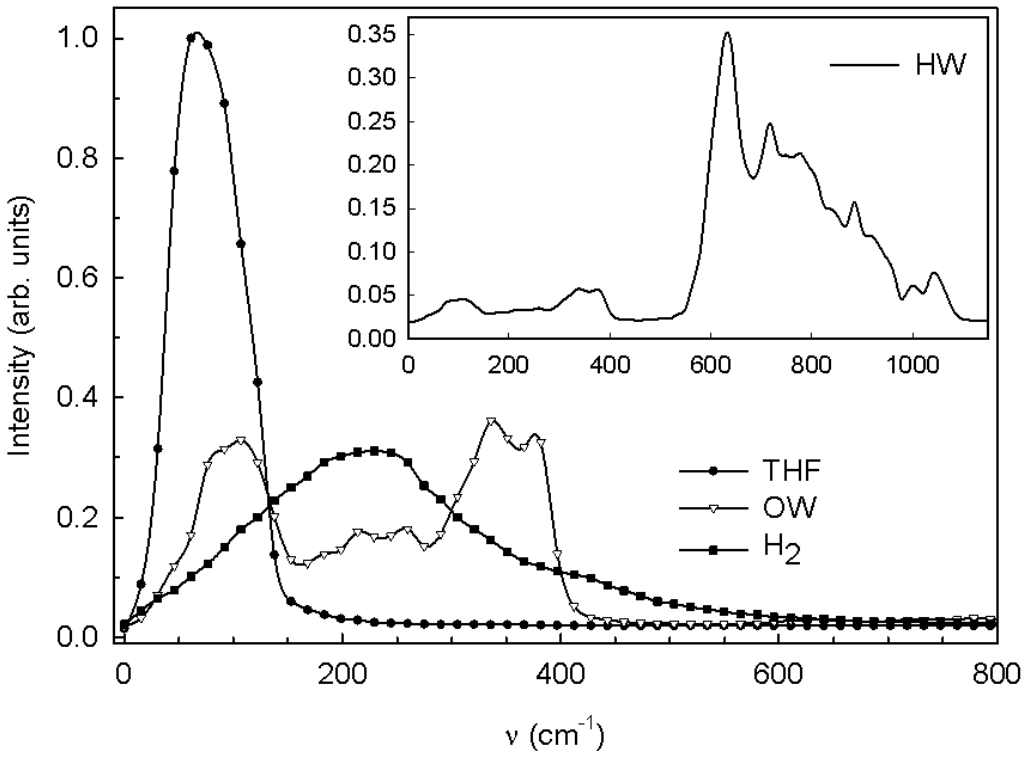

Fig. 2a FT-VACF 1s1l SPC/E 30K

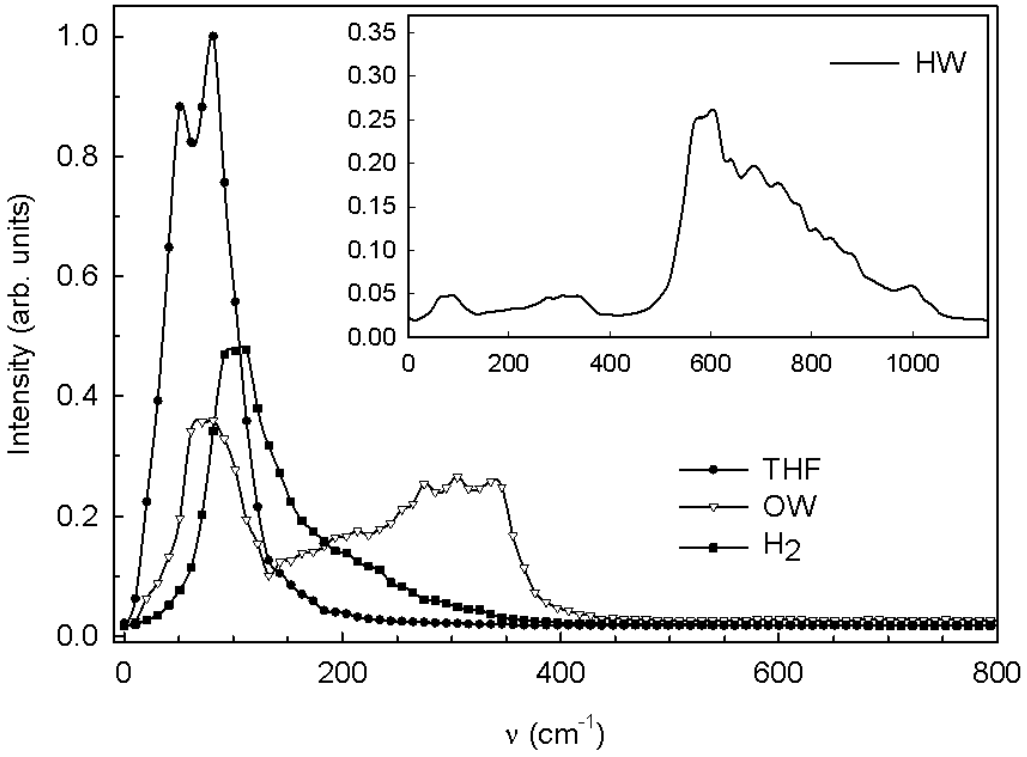

Fig. 2b FT-VACF 1s1l SPC/E 200K

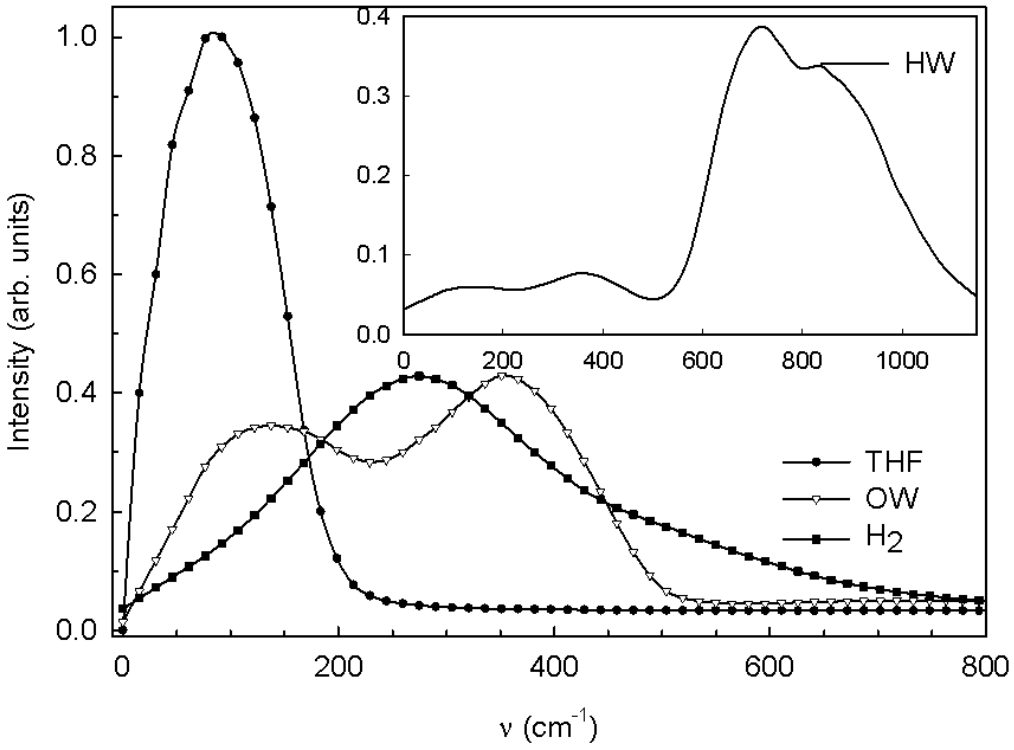

Fig. 3a FT-VACF 1s1l TIP4P-2005 30K

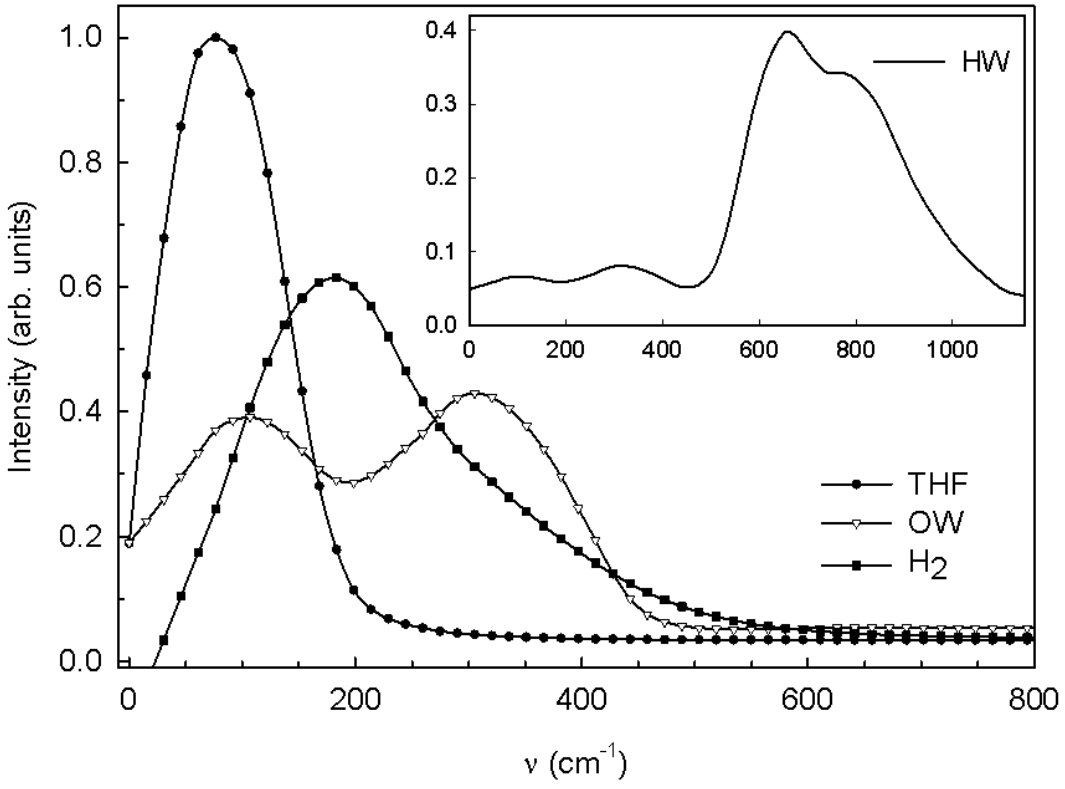

Fig. 3b FT-VACF 1s1l TIP4P-2005 200K

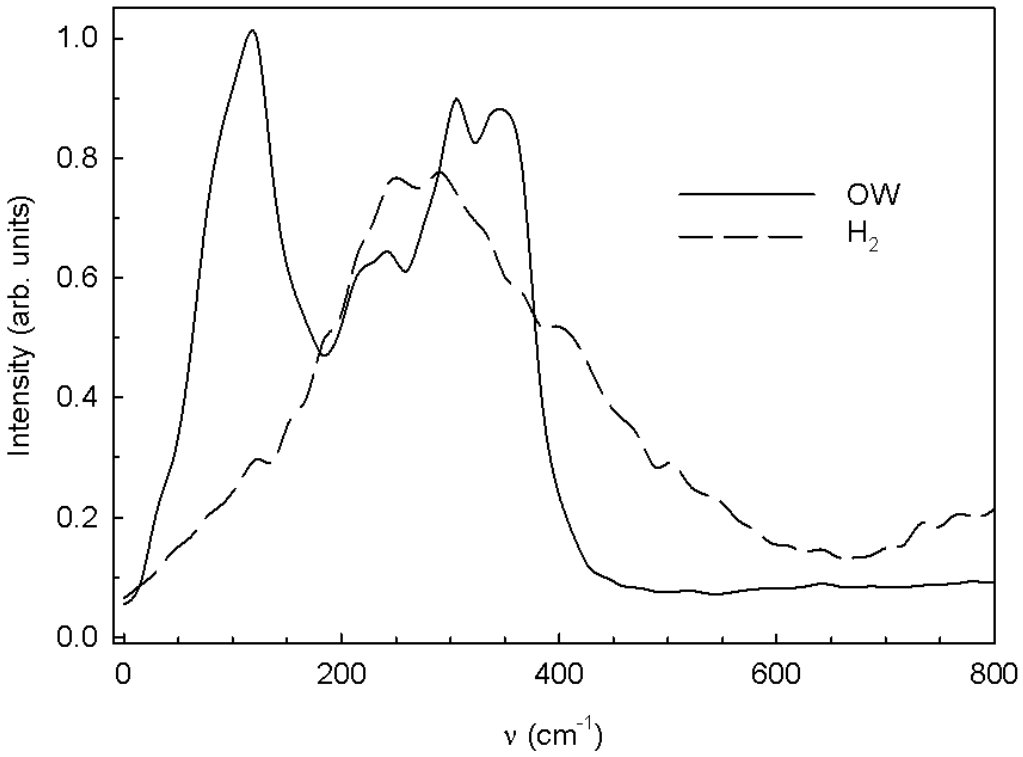

Fig. 4a FT-VACF 2s1l SPC/E 30K OW vs. H_2

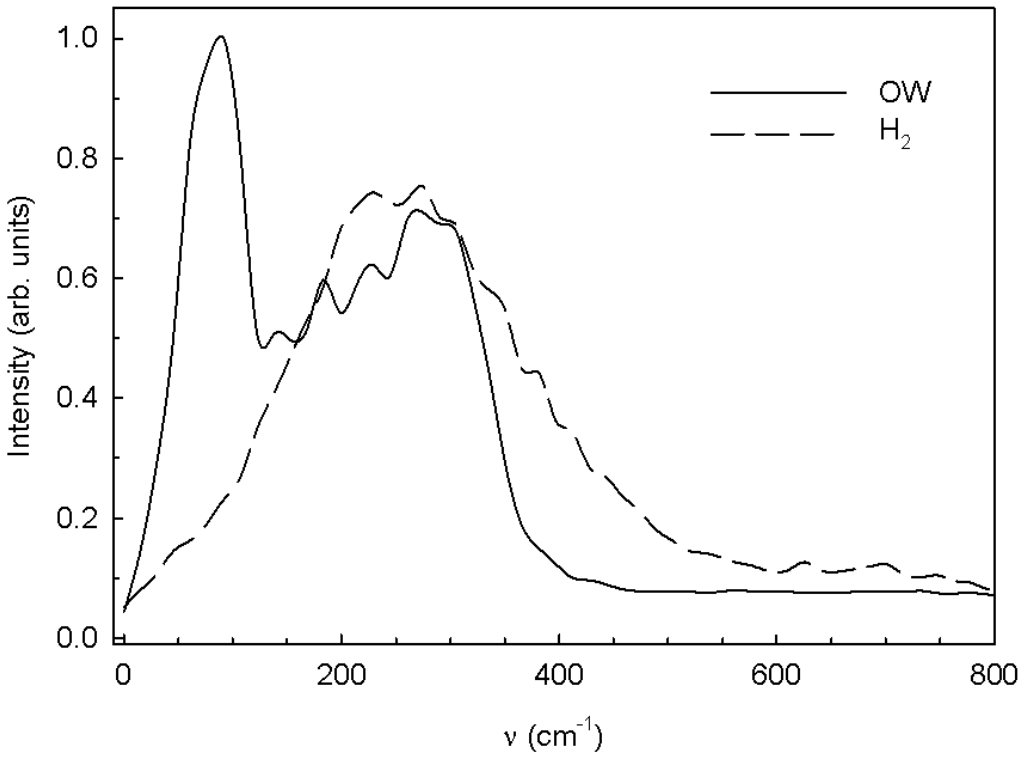

Fig. 4b FT-VACF 2s1l SPC/E 200K OW vs. H_2

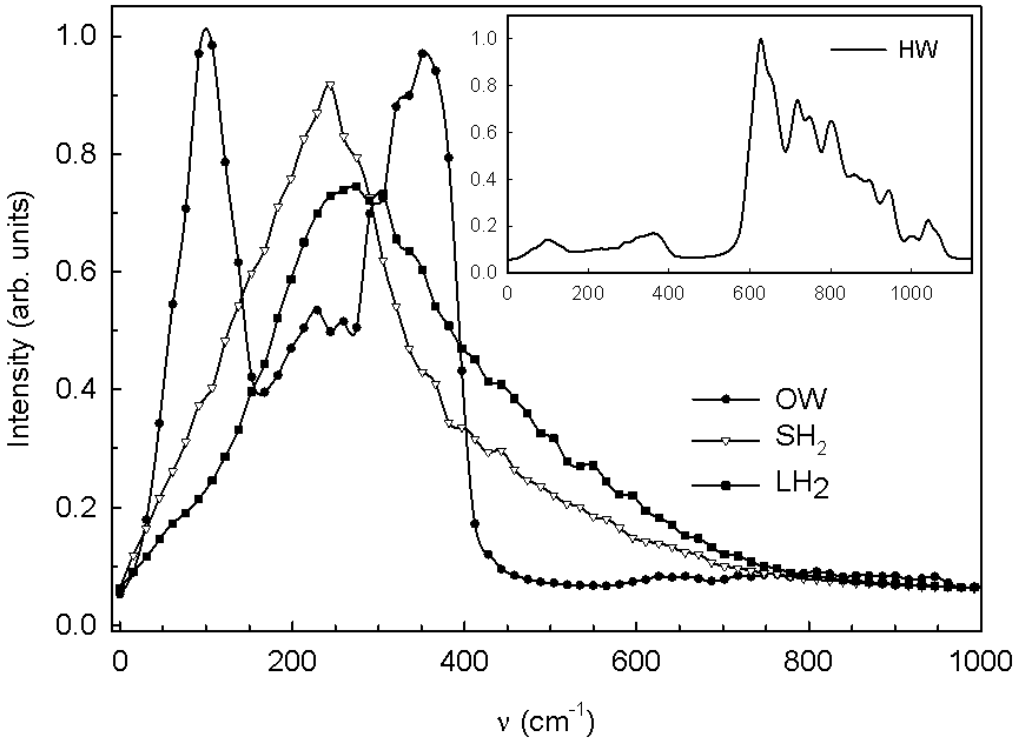

Fig. 5a FT-VACF 1s4l SPC/E 30K

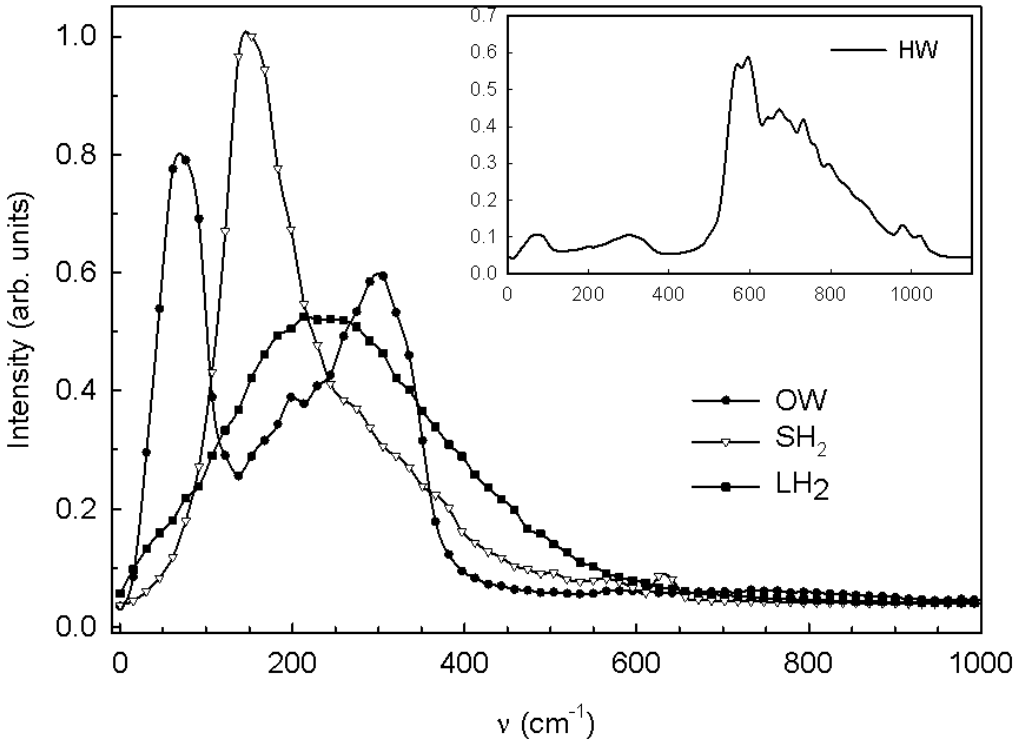

Fig. 5b FT-VACF 1s4l SPC/E 200K

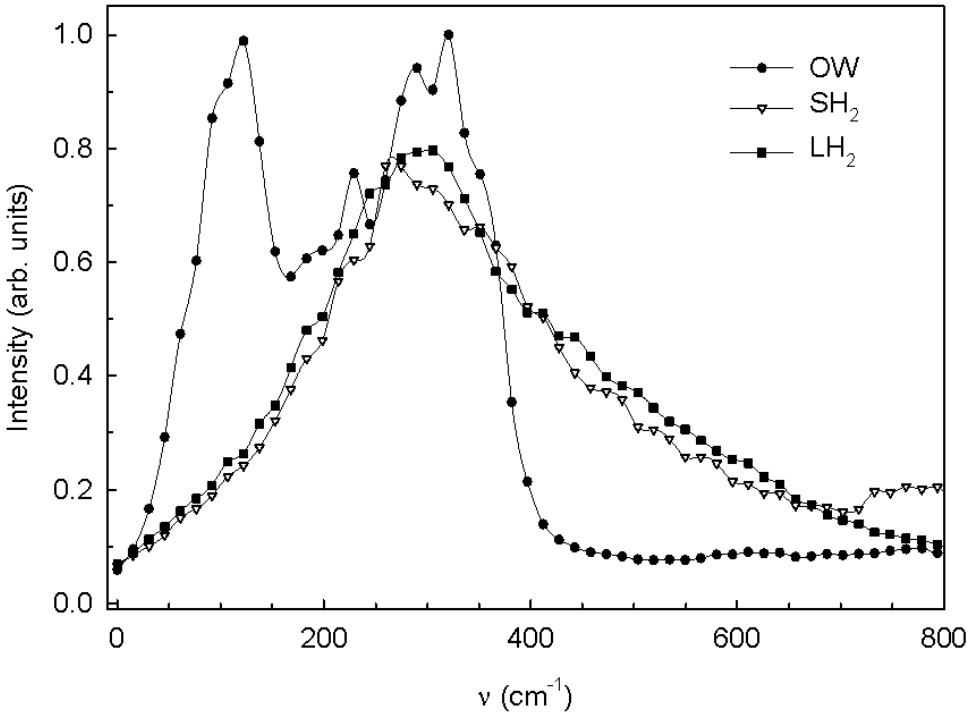

Fig. 6a FT-VACF 2s4l SPC/E 30K

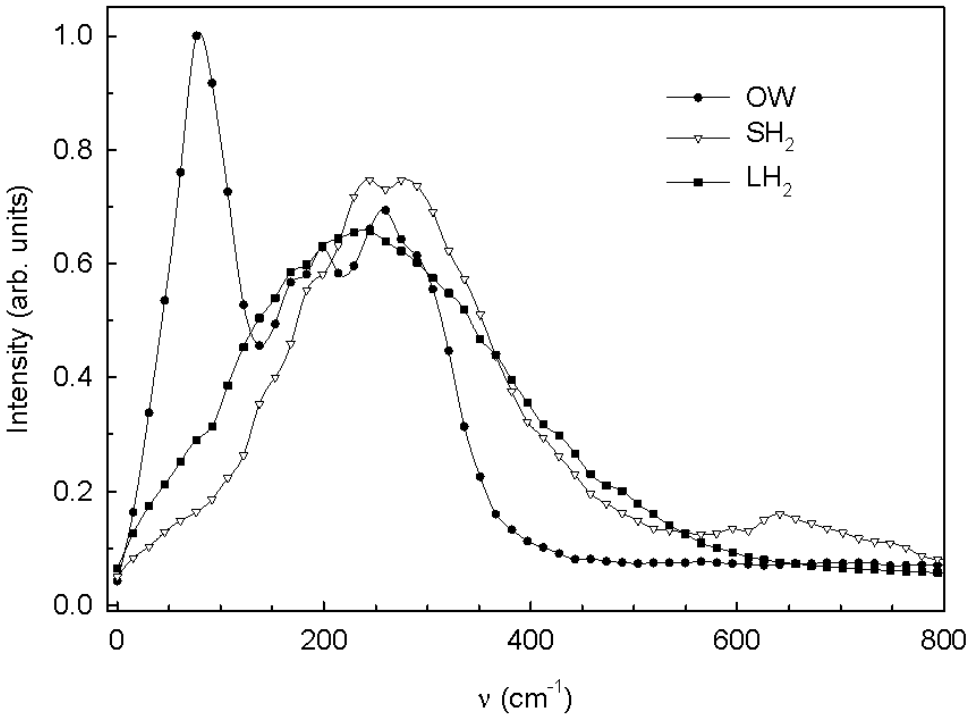

Fig. 6b FT-VACF 2s4l SPC/E 200K

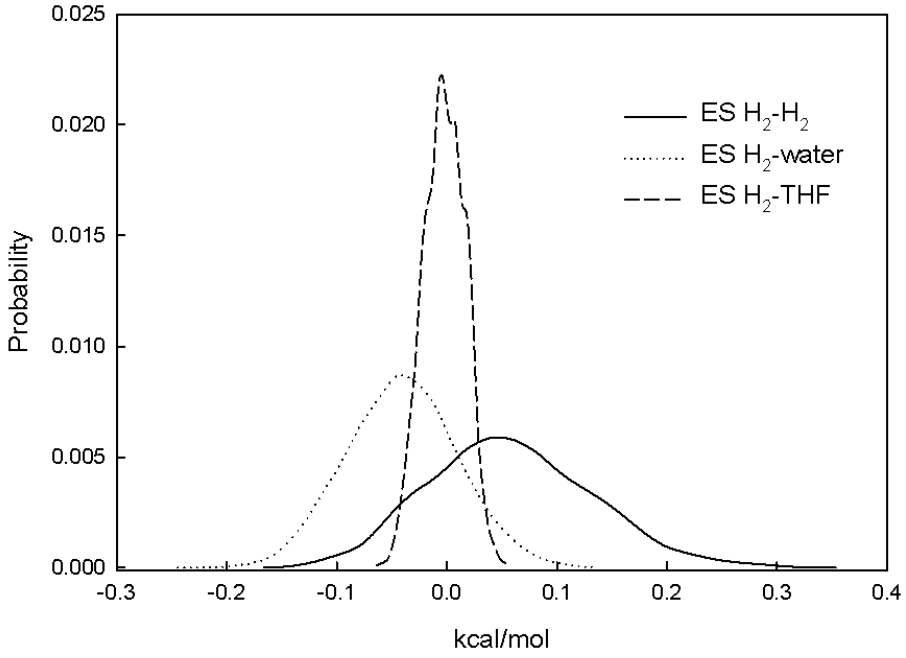

Fig. 7a H_2 electrostatic energies for the 1s1l system at 30 K with SPC/E

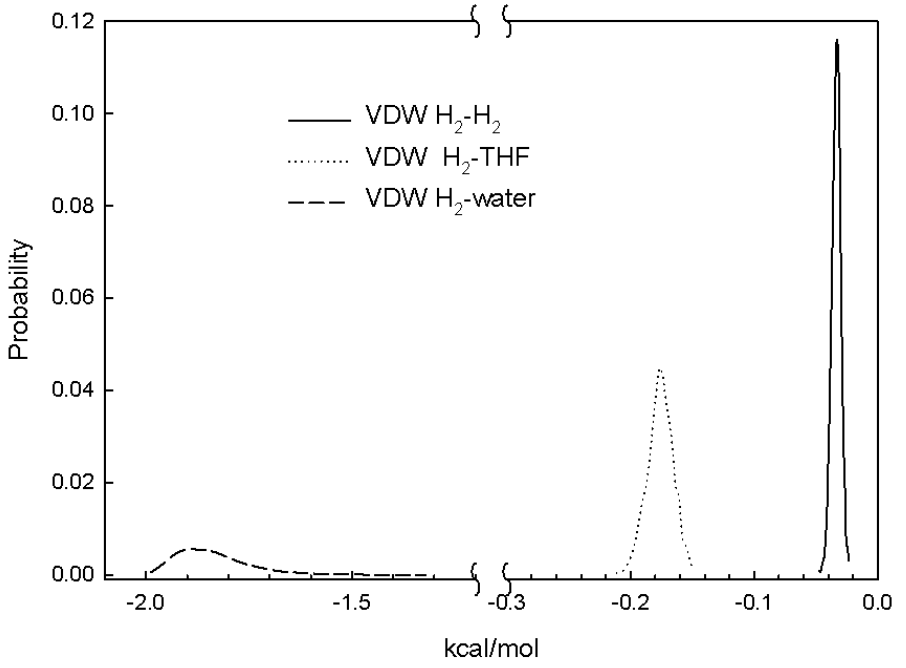

Fig. 7b H_2 van der Waals energies for the 1s1l system at 30 K with SPC/E

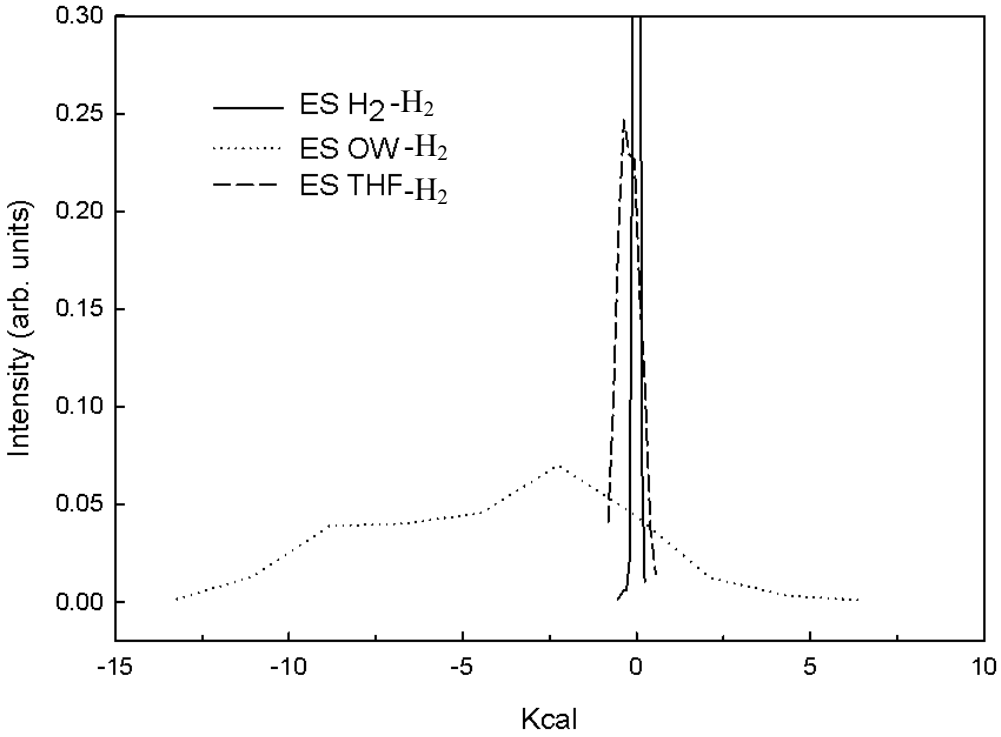

Fig. 8a THF electrostatic energies for the 2s1l system at 200K with TIP4P-2005

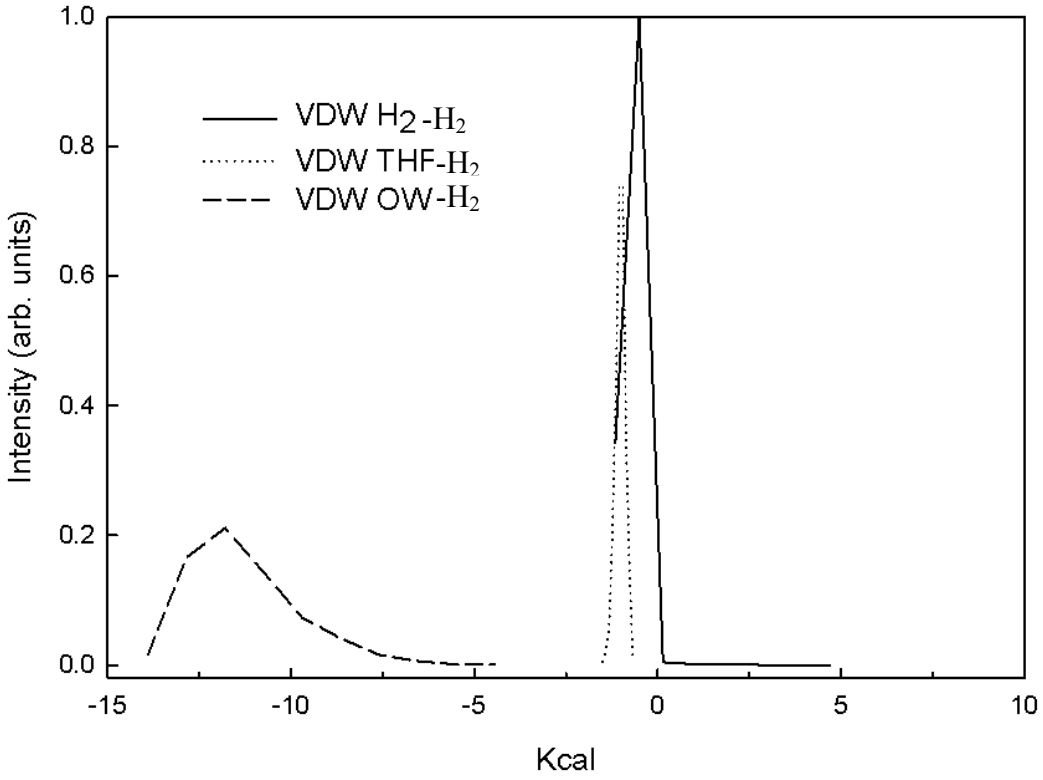

Fig. 8b THF van der Waals energies for the 2s1l system at 200K with TIP4P-2005

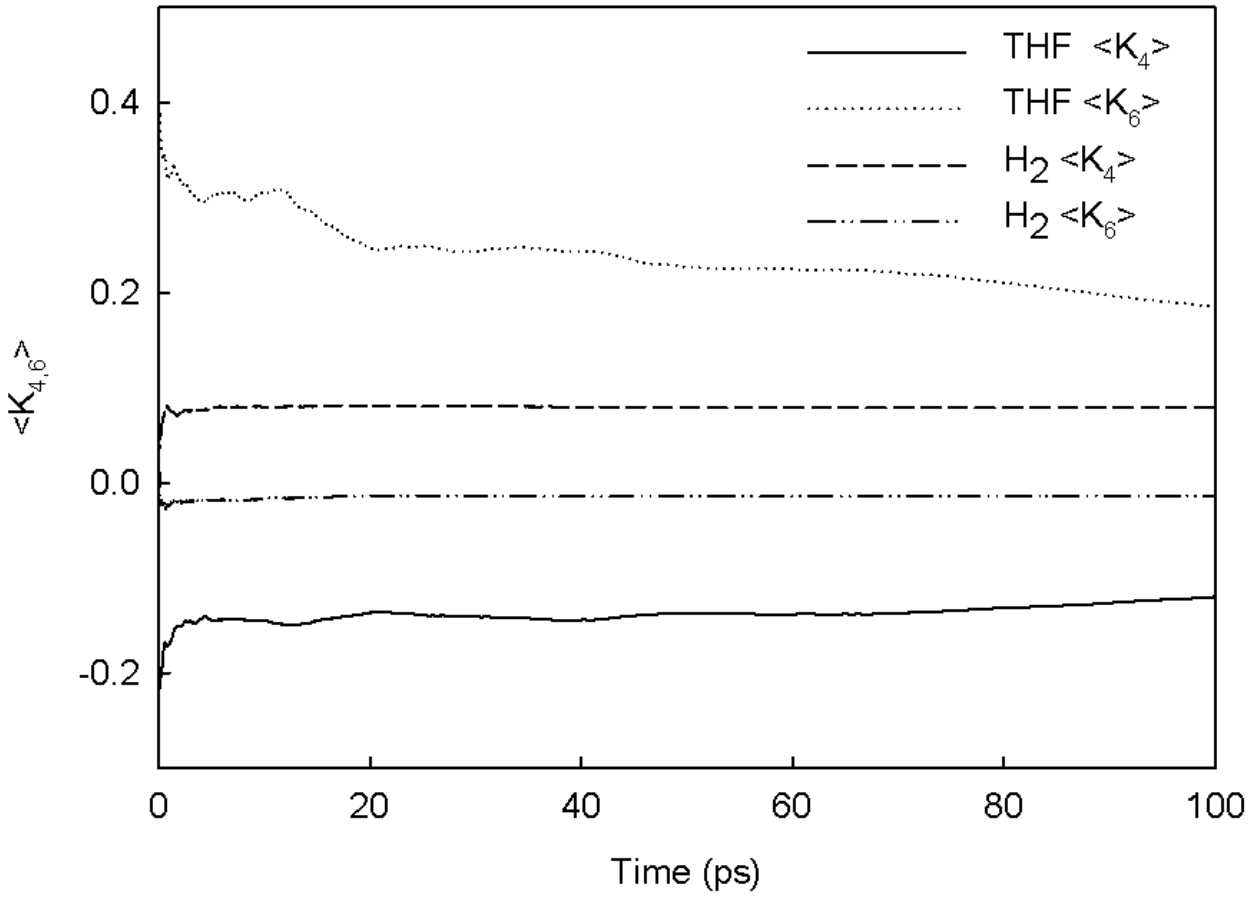

Fig. 9 Kubic harmonics, 2s11 TIP4P-2005 200K